

# A simple conceptual model to interpret the 100 000 years dynamics of paleo-climate records

C. S. Quiroga Lombard<sup>1</sup>, P. Balenzuela<sup>1,2</sup>, H. Braun<sup>3,\*</sup>, and D. R. Chialvo<sup>2</sup>

<sup>1</sup>Departamento de Física, Facultad de Ciencias Exactas y Naturales, Universidad de Buenos Aires, Pabellón 1, Ciudad Universitaria (1428), Buenos Aires, Argentina

<sup>2</sup>Consejo Nacional de Investigaciones Científicas y Técnicas (CONICET), Av. Rivadavia 1917 (1033), Buenos Aires, Argentina

<sup>3</sup>Heidelberg Academy of Sciences and Humanities, University of Heidelberg, Heidelberg, Germany

\* now at: Center for Ice and Climate, University of Copenhagen, Copenhagen, Denmark

Received: 15 June 2010 – Revised: 27 August 2010 – Accepted: 2 September 2010 – Published: 13 October 2010

**Abstract.** Spectral analyses performed on records of cosmogenic nuclides reveal a group of dominant spectral components during the Holocene period. Only a few of them are related to known solar cycles, i.e., the De Vries/Suess, Gleissberg and Hallstatt cycles. The origin of the others remains uncertain. On the other hand, time series of North Atlantic atmospheric/sea surface temperatures during the last ice age display the existence of repeated large-scale warming events, called Dansgaard-Oeschger (DO) events, spaced around multiples of 1470 years. The De Vries/Suess and Gleissberg cycles with periods close to  $1470/7$  ( $\sim 210$ ) and  $1470/17$  ( $\sim 86.5$ ) years have been proposed to explain these observations. In this work we found that a conceptual bistable model forced with the De Vries/Suess and Gleissberg cycles plus noise displays a group of dominant frequencies similar to those obtained in the Fourier spectra from paleo-climate during the Holocene. Moreover, we show that simply changing the noise amplitude in the model we obtain similar power spectra to those corresponding to GISP2  $\delta^{18}\text{O}$  (Greenland Ice Sheet Project 2) during the last ice age. These results give a general dynamical framework which allows us to interpret the main characteristic of paleoclimate records from the last 100 000 years.

i.e., the De Vries/Suess, Gleissberg and Hallstatt cycles. The origin of the others remains uncertain. On the other hand, climate records from the North Atlantic region show prominent temperature variations during the last ice age associated with transitions between cold stadials and warm interstadials, the so-called Dansgaard-Oeschger events. The recurrence time between these events varied considerably, ranging from  $\sim 1$  to 12 kyr during the last 90 kyr (Bond et al., 1999). The variability of the pacing was greatly reduced between 25 and 60 kyr BP (Before Present), when the spacing between the warming events was  $\sim 1 - 5$  kyr. In the GISP2 data, the interval 12–50 kyr BP shows an apparently significant spectral component corresponding to a period of about 1470 years (Schulz, 2002). Recently (Braun et al., 2005) it has been proposed that the De Vries/Suess and Gleissberg cycles with periods close to  $1470/7$  ( $\sim 210$ ) and  $1470/17$  ( $\sim 86.5$ ) year could be responsible of these variations. This hypothesis was tested by forcing a coupled climate system model CLIMBER-2 (version 3) with oscillations of 210 and 87 years cycles in the influx of fresh water into the Northern-Atlantic and reanalyzed in a nonlinear simple conceptual model (Braun et al., 2007, 2008) driven by two sinusoidal tones with the mentioned frequencies. The success of these results, however, were restricted to DO events during the interval 12–50 kyr BP where they show to be often spaced by 1470 years.

A global perspective of the climate records from the North Atlantic region for the last ice age suggest that temperature variations are the result of the switching between two stable states (a warm and a cold one) with different dynamical regimes, being the quasi-periodicity of about 1470 years during the interval 12–50 kyr BP one of those dynamical regimes. The hypothesis underlying this work is that the existence of a driving force composed by the near De-Vries/Suess and Gleissberg cycles plus a Gaussian noise rule

## 1 Introduction

Spectral analyses performed on records of cosmogenic nuclides (ZhiQiang et al., 2007; Sonett et al., 1990; Stuiver and Braziunas, 1993; Peristykh and Damon, 2003) reveal a group of dominant spectral components during the Holocene period. Only a few of them are related to known solar cycles,



Correspondence to: P. Balenzuela  
(balen@df.uba.ar)

the transitions between both states. If so, this simple scheme should explain the temperature variations in the whole ice age and the effects of the solar forcing should be noticeable also during the Holocene when DO events were absent.

To test this hypothesis we propose a new conceptual model based on the key assumptions of the CLIMBER-2 and the information obtained after having analyzed two climate records, the GISP2  $\delta^{18}\text{O}$  and  $^{14}\text{C}$  measurements from tree rings. These records are used as proxies for temperature and solar activity, respectively.

We will show that the model is able to reproduce the main features of the Fourier spectra of the different stages of Greenland temperature variations and also lets to a plausible explanation of the frequency spectra obtained from the  $^{14}\text{C}$  record.

This paper is organized as follows: in the next section we will show the Fourier spectra analysis for the GISP2  $\delta^{18}\text{O}$  and the IntCal04  $^{14}\text{C}$  records. In Sect. 3 we develop the model used to obtain time series comparable to the experimental data. In Sect. 4 we analyze the time series produced by the model and compare with GISP2  $\delta^{18}\text{O}$  and  $^{14}\text{C}$  records. Finally, we discuss the results in the conclusion section.

## 2 Holocene time series analysis

In order to capture the main frequencies present during this age, we analyze two different registers: the IntCal04  $^{14}\text{C}$  record and the last 11 000 years of the GISP2 record. The first one contains the estimated partial flux density of  $^{14}\text{C}$  (in atoms per second per square-meter) (“cal BP”), produced by cosmic rays and nitrogen. This partial flux is modulated by solar activity, i.e., by changes in the magnetic field of the Sun (the partial flux is higher in times of low solar activity), and it is a standard record to conclude about solar variability in the past. However, it should be noticed that IntCal04  $^{14}\text{C}$  record is also likely to be influenced by other factors such variability of the earth’s magnetic field or ocean variability (Stuiver and Braziunas, 1993) which may affect the concentration of  $^{14}\text{C}$  in atmosphere and therefore in tree rings. The time resolution of this data is 5 years, i.e., there are about  $N = 2276$  data points. The data are calculated from  $^{14}\text{C}$  measurements in precisely-dated, high resolution tree rings. The second record contains the  $\delta^{18}\text{O}$  variations from the GISP2 ice core, a proxy for temperature, for the past 11 000 years aprox. Because the time step is not equidistant, we did a linear interpolation in order to have an almost uniform time interval necessary to perform our analysis. The time interval after interpolation is  $T = 4$  years with  $N = 2738$  data points. The original time interval distribution is peaked around 15 years aprox.

We performed a Fourier spectra analysis for both records. Figure 1 shows the experimental signals (panels a and c) and their frequency spectra (panels b and d). In both analyses we have added around  $5N$  zeros and used the Hanning function in order to have a better resolution and improving the results.

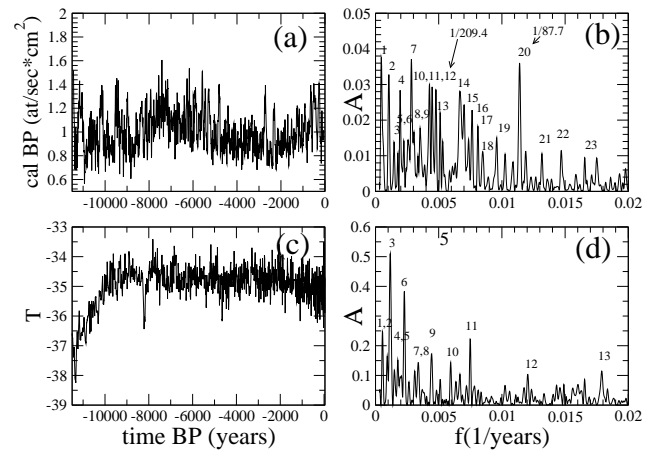


**Fig. 1.** Panel (a):  $^{14}\text{C}$  record (proxy for solar activity) and panel (b) its frequency spectra. The periods (in years) associated with the labeled frequencies are: (1) 2276; (2) 948.3; (3) 564.3; (4) 513.4; (5) 446.3; (6) 388; (7) 351.9; (8) 328.3; (9) 283.3; (10) 233.8; (11) 223.1; (12) 209.4; (13) 195.6; (14) 149.7; (15) 142.5; (16) 135.7; (17) 130.8; (18) 117.9; (19) 104.2; (20) 87.7; (21) 75.7; (22) 68; (23) 60.4. Panel (c): interpolated GISP2 record for the past  $\sim 11\,000$  years and panel (d) its frequency spectra. The periods (in years) associated with the labeled frequencies are: (1) 1789; (2) 1079; (3) 860; (4) 667; (5) 566; (6) 438; (7) 322; (8) 295; (9) 225; (10) 168; (11) 133; (12) 83; (13) 56.

We have labeled the 23th and 13th most prominent peaks of the  $^{14}\text{C}$  and the GISP2  $\delta^{18}\text{O}$  Fourier spectra. These peaks are those which amplitudes are greater than two standard deviation of the spectral amplitudes distribution.

A visual inspection of these figures give us the following results:

- The periods with greater amplitude in the Fourier transform of  $^{14}\text{C}$  register are 2276, 948.3, 513.4, 351.9, 233.8, 223.1, 209.4, 195.6, 149.7, 142.5, 135.7, 130.9, 87.7 years.
- About half of them coincide with previously reported analyses performed with different methods (ZhiQiang et al., 2007; Sonett et al., 1990), namely: **948.3 (2)**, **513.4 (4)**, **351.9 (7)**, **209.4 (12)**, **149.7 (14)**, **130.9 (17)**, **87.7 (20)** years. For this reason we will consider this list as the most important periods and will be taken as a reference for the simulation analysis.
- Nine spectral peaks of  $\delta^{18}\text{O}$  record are close (within a 10% percentage error) to values found in the  $^{14}\text{C}$  record. Seven of them (860 (3), 566 (5), 322 (7), 225 (9), 168 (10), 133 (11), and 83 (12)) belong to the group of the mentioned important periods.
- We found the presence of 87.7, 209.4, and 2276 years periods than could be associated to the Gleissberg ( $\sim 88$  years), De Vries/Suess ( $\sim 207$  years) and Hallstatt

( $\sim 2300$  years) cycles (Sonett et al., 1990; Wagner et al., 2001; Stuiver and Braziunas, 1993). Also  $\sim 950$  and  $\sim 550$  years were reported as related to solar cycles (Dima and Lohmann, 2009).

- The others dominants spectral components could not be related to solar cycles.

These analyses give us a experimental framework where we can elaborate a model and analyze the generated results.

### 3 The model

If we look at the GISP2  $\delta^{18}\text{O}$  records during last ice age it can be observed that the temperature variations seem to be the result of the switching between two stable states in the earth climate, i.e., a warm and a cold one. In Braun et al. (2005) it was hypothesized that a solar forcing driven by the Gleissberg ( $\sim 88$  years) and the De Vries/Suess ( $\sim 207$  years) cycles could be responsible for such transitions (called DO events) given that they could cause a 1470 year resonance. The work assumes that periodic solar variations promote transitions between a stadial (“cold”) and interstadial (“warm”) mode of the North Atlantic thermohaline circulation (THC), being the 1470 years regularity in Greenland temperature fluctuations a particular consequence of the solar forcing.

In Braun et al. (2007) the authors explore the idea that the main mechanism underlying the DO events is a consequence of two well-known properties of the THC: its long characteristic timescale and the high degree of nonlinearity (that is, the threshold character) inherent in the transitions between the two modes of the THC. With this goal they analyzed a very simple conceptual model that incorporates these two properties and is able to mimic the key features of CLIMBER-2. The general idea of this model is that DO events represent highly nonlinear switches between two different climate states corresponding to the glacial and modern modes of the THC.

If the previous hypotheses are true, the same periodic forcing behind the transitions between warm and cold states during the last ice age should be present in the global climate also when transitions are absent. Following this approach we analyze a new conceptual model based in the main characteristics used to develop the conceptual model previously mentioned:

1. The existence of two states, the cold and the warm one.
2. The states represent two different modes of operation of the thermohaline circulation (THC) in the North Atlantic region; the modern and the glacial one.
3. The model is forced by a solar process with the frequencies of the De Vries/Suess and Gleissberg cycles ( $\sim 207$  and  $\sim 87$  years, respectively) and a stochastic component.

4. A transition between states takes place each time a certain threshold is crossed.
5. With every transition the threshold overshoots and afterwards approaches equilibrium following a millennial time scale relaxation process.
6. During the Holocene the periodic forcing is not able to produce transitions and the climate temperature remains in the warm state.

For accomplishing these assumptions we will consider the dynamic of a system submitted to a periodic forcing (with the frequencies mentioned before) in a double well potential and a stochastic component representing all the degrees of freedom which are not explicitly taken into account.

Simulations with an ocean-atmosphere model suggest that the barrier generated by the potential decreases exponentially with a time constant of  $\sim 1200$  years if the system is in the cold state and  $\sim 800$  years if it is in the warm state (Braun et al., 2007, 2008). The forcing will be composed of the two frequencies related to the De Vries/Suess and Gleissberg cycles. We take their relative amplitude and phase from the  $^{14}\text{C}$  analysis. Finally, the stochastic component will be implemented as a Gaussian noise of zero mean value and amplitude  $D$ .

This model is represented in the following set of differential equations,

$$\dot{x} = \frac{1}{a} \left[ y \cdot (x - x^3) + f(t) + D\sqrt{a}\xi(t) \right] \quad (1)$$

$$\dot{y} = -\frac{y}{\tau_s} + \delta_s, \quad (2)$$

where  $y \cdot (x - x^3) = -\frac{dV}{dx}$  and  $V(x)$  is a double well potential with a potential barrier following the dynamics of the  $y$  variable.  $f(t) = F \cdot (\cos(2\pi f_1 t + \phi_1) + \alpha \sin(2\pi f_2 t + \phi_2))$  represents the solar forcing whose main parameters, amplitude  $F$ , frequencies  $f_1$  and  $f_2$ , phases  $\phi_1$  and  $\phi_2$  and  $\alpha$  the relative amplitude of both tones, were taken from  $^{14}\text{C}$  time series analysis. The term  $D\xi(t)$  stands for a white noise of zero mean and amplitude  $D$  process and  $a$  is a scaling constant. In the equation for threshold dynamics,  $\tau_s$  and  $\delta_s$  are the characteristic time decay and asymptotic threshold respectively ( $s = 1(-1)$  for warm (cold) state).

In the simulations shown in this paper we took  $f_1 = 1/209.4 \text{ years}^{-1}$ ,  $f_2 = 1/87.7 \text{ years}^{-1}$ ,  $\phi_1 = -0.1483$ ,  $\phi_2 = -0.5255$ ,  $\alpha = 1.1303$ . All these values were taken from the Fourier analysis of  $^{14}\text{C}$  time series performed above. The value of the constant  $a = 7.7986$  was taken in order to adjust the characteristic times of the model to the scale of experimental data and the values  $\tau_{-1} = 1200$  and  $\tau_1 = 800$  was chosen like in (Braun et al., 2007). We also set  $\delta_s = 0.8/\tau_s$  and  $y(0) = 1.5$ .

We will consider that the system is in the warm state when the  $x$  variable oscillates around the  $+1$  fixed point. On the contrary, when the  $x$  variable oscillates around the  $-1$  fixed point we will consider that our system is in the cold state.

This system was integrated following an Euler method (García-Ojalvo and Sancho, 1999) with a time step of  $h = a/10$ . In order to implement the overshooting of the threshold after every transition, the variable  $y$  is reseted to its initial value every time the system makes a transition from one stable state to the other.

In this model, the variable  $x$  is an observable that represents the state of the climate system. For simplicity, we will assume that  $x$  represents the temperature (reflected in the  $\delta^{18}\text{O}$  register) and also (at least for the Holocene) the interaction with solar activity reflected in  $^{14}\text{C}$  record. This assumption is of course an oversimplification, because the connection between the  $\delta^{18}\text{O}$  and  $^{14}\text{C}$  variable is not well known. Thus, considering a linear relation between both of them is the simplest possible choice, at least for the Holocene where massive temperature jumps are absent. The election of such linear relation is also supported by similarities found between the Holocene  $^{14}\text{C}$  record and climate records of various origins (Stuiver et al., 1997; O'Brien et al., 1995; Crowley et al., 1993; Karlen and Kuylensstierna, 1996). In particular in Stuiver et al. (1997) the authors suggest that the overall agreement between the timing, estimated order of magnitude temperature change, and phase lag of the  $\delta^{18}\text{O}$  and  $^{14}\text{C}$  signals is suggestive of solar forcing of Greenland climate for the current millennium.

A key property in the response of these kinds of models when driven by a periodic forcing is that transitions between both stable states depends strongly on the relation between the forcing amplitude  $F$ , the barrier high (proportional to  $y(t)$ ) and the noise amplitude  $D$  (Gammaitoni et al., 1998). However, the dynamical backbone that rules the transitions could be analyzed in absence of noise. In Fig. 2 we give a brief sketch of the dynamics of the model. In panel a, we analyze the dynamics of the transitions by plotting the maximum oscillation amplitude  $A = \max(x(t)) - \min(x(t))$  as a function of the forcing amplitude  $F$ . This plot allows us to identify the onset of transitions in absence of noise (labeled 2 in panel a) which is around  $F = 0.2265$ . For low forcing amplitudes (label 1 in the same panel,  $F = 0.1$ ) the system oscillates around one of the stable states. In this case the frequency spectra is dominated by the input frequencies  $f_1 = 1/209.4 \text{ years}^{-1}$  and  $f_2 = 1/87.7 \text{ years}^{-1}$  as can be observed in panel b. For large forcing amplitudes (label 3 in Fig. 2,  $F = 0.31$ ) the particle oscillates between both stable states and the transitions are spaced by the distance between the forcing function's global maxima. Its frequency spectra and temporal series are display in panel f. The richest dynamics scenario for this model occurs at the onset of transitions (label 2 in Fig. 2) as we observe in panel d. Panels c and e show the temporal characteristics of the forcing function and its autocorrelation function, respectively.

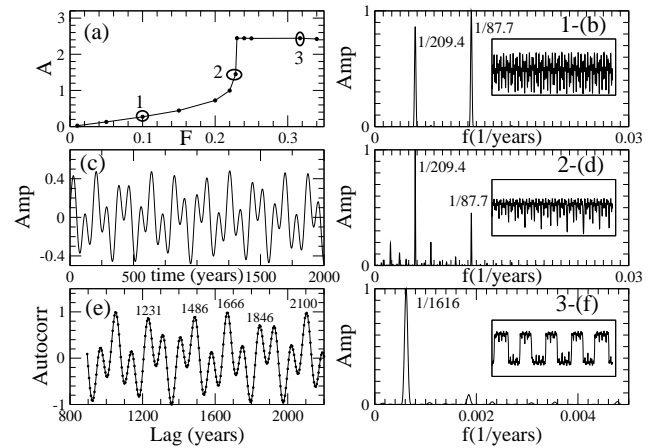


**Fig. 2.** Panel (a): maximal oscillation amplitude  $A = \max(x(t)) - \min(x(t))$  as a function of the forcing amplitude  $F$  in absence of noise. Labels 1, 2 and 3 show the three distinct regimes. Panels (b), (d) and (f): frequency spectrum of  $x(t)$  and time series (inset) for low (label 1), onset of transitions (label 2) and high (label 3) forcing amplitudes, respectively. The forcing amplitudes for each panel are:  $F = 0.1$  for panel (b),  $F = 0.2265$  for panel (d) and  $F = 0.31$  for panel (f). Panel (c) and (e): forcing function for the bistable model  $f(t) = F \cdot (\cos(2\pi f_1 t + \phi_1) + \alpha \sin(2\pi f_2 t + \phi_2))$ .  $f_1 = 1/209.4 \text{ years}^{-1}$ ,  $f_2 = 1/87.7 \text{ years}^{-1}$ ,  $\phi_1 = -0.1483$ ,  $\phi_2 = -0.5255$ ,  $\alpha = 1.1303$  and its autocorrelation function, respectively.

## 4 Results

### 4.1 The Holocene

Our hypothesis is that the observed frequencies in the Holocene time series analysis ( $\delta^{18}\text{O}$  and  $^{14}\text{C}$ ) are the result of the interaction between the forcing  $f(t)$  and the strong nonlinearities of the climate system (represented by the potential in our model). As we have seen in the previous section, the richest dynamical scenario takes place at the onset of transitions. In order to find when the dynamics of the model is close to the Holocene records, we place the system in the onset of the transitions and minimize the distance between the main peaks of the simulations Fourier spectra and the spectral components of the seven main frequencies observed in the  $^{14}\text{C}$  record. We use the same parameters value described in previous section and we use  $F = 0.2265$ .

The procedure was as follows: given the specified set of parameters values, we performed an ensemble of  $N_{\text{event}} = 100$  simulations of  $\sim 11\,000$  years (a time interval similar to the experimental data time interval). For each event, we obtained the Fourier spectra and calculated the root mean square (RMS) distance between the components that minimize this distance with the seven most important

experimental frequencies components,

$$d^j = \sqrt{\frac{1}{N_{\text{dim}}} \sum_i^{N_{\text{dim}}} \frac{(s_i^j - e_i)^2}{e_i^2}}, \quad (3)$$

where  $(e_1, \dots, e_{N_{\text{dim}}})$  is the vector composed by the seventh experimental frequencies and  $(s_1^j, \dots, s_{N_{\text{dim}}}^j)$  is the vector containing the spectral components that minimize the RMS for the  $j$ -th event of the simulation. To find the best agreement between experimental data and simulations we varied the noise amplitude  $D$  in order to minimize this distance. In Fig. 3 we plot the ensemble-average ( $\langle d \rangle$  in panel a) and minimum distance ( $\langle d \rangle_{10 \text{ min}}$  and  $d_{\text{min}}$  in panel b) between the simulated and experimental frequency spectra as a function of noise amplitude, together with the simulated time series (panel c) and Fourier spectra (panel d). The minimum value of the ensemble-average distance indicates the value of the noise amplitude at which most of the simulated frequencies components best fit the experimental frequencies, considering the main spectral components. The broader range observed in the minimum distance indicates that a good fit between frequencies can be found in a wide range of noise showing that this is a robust feature of the system. The simulated time series and its Fourier spectra are the ones corresponding to the minimum distance.

We can observe that others frequencies appear in the simulation's Fourier spectra together with the seven main frequencies. This is a consequence of the interplay between the forcing and the non-linearities present near the onset of transitions. Notoriously, these spectral components are also present in the analysis of  $^{14}\text{C}$  and GISP2  $\delta^{18}\text{O}$  during the Holocene. We give a full comparison in Table 1.

Even though we have found important similarities between the experimental and simulated frequencies components, the differences in amplitude are evident. Also there are spectral components in both records that this simple model is unable to reproduce. These differences can be understood if we take into consideration that our model presents a very simple non-linear interaction between the forcing function and the threshold. Nevertheless, this simple interaction allows us to explain the presence of some of the most important experimental frequencies components.

#### 4.2 The ice age

The results of the previous section show that this simple model is able to explain the presence of the main frequencies in the Fourier spectra of paleo-temperature and  $^{14}\text{C}$  records during the Holocene. If the underlying hypothesis is true, the same description should be able to reproduce similar results during the last ice age. In what follows we show that by keeping the same values of the model's parameters and simply changing the noise amplitude the model is able to reproduce the main features of the GISP2  $\delta^{18}\text{O}$  record Fourier spectra.

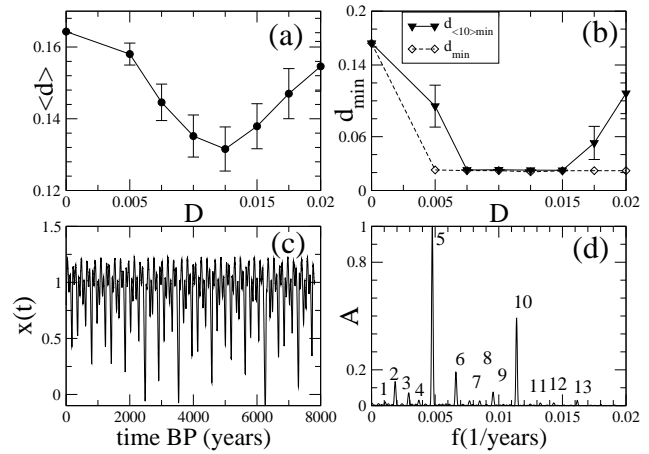


**Fig. 3.** Holocene: ensemble-average (panel a) minimum distance and average over the ten smallest distances (panel b) between simulations and experimental spectra as a function of noise amplitude, together with the simulated time series (panel c) and Fourier spectra (panel d). The noise amplitude used in panels c) and d) is 0.0125. The periods associated with the labeled frequencies are: (1) 928, (2) 540, (3) 341, (4) 270, (5) 209.4, (6) 150.8, (7) 129.8, (8) 117.8, (9) 104.6, (10) 87.7, (11) 75.4, (12) 69.7, (13) 61.8.

**Table 1.** Main periods obtained from the single ensemble of the simulation with  $F = 0.2265$  and  $D = 0.0125$  (first column). Periods found in the  $^{14}\text{C}$  (second column) and  $\delta^{18}\text{O}$  (third column) records that can be related to the simulation results. We highlight the periods described in other works (ZhiQiang et al., 2007; Sonett et al., 1990) and considered important in our analysis.

| Simulation<br>(in years) | $^{14}\text{C}$<br>(in years) | GISP2 $\delta^{18}\text{O}$<br>(in years) |
|--------------------------|-------------------------------|---|
| 928                      | <b>948.3</b>                  | 860                                       |
| 540                      | <b>513.4</b>                  | 566                                       |
| 341                      | <b>351.9</b>                  | 322                                       |
| 270                      | 283.3                         | 295                                       |
| 209.4                    | <b>209.4</b>                  | 225                                       |
| 150.8                    | <b>149.7</b>                  | 168                                       |
| 129.8                    | <b>130.8</b>                  | 133                                       |
| 117.8                    | 117.9                         | –   |
| 104.6                    | 104.2                         | –   |
| 87.7                     | <b>87.7</b>                   | 83  |
| 75.4                     | 75.7                          | –   |
| 69.7                     | 68                            | –   |
| 61.8                     | 60.4                          | 56  |

First of all, the GISP2  $\delta^{18}\text{O}$  record extends approximately over the past 110 000 years. We split the analysis of this records in three parts: time interval I ( $\sim 110\,000$ – $50\,000$  years BP) corresponds to the early ice age where DO events were sporadic. Time interval II ( $\sim 50\,000$ – $11\,500$  years BP) corresponds to late ice age where DO events are spaced by near-multiples of  $\sim 1470$  years (Schulz, 2002). The time interval labeled as III corresponds to the Holocene and it was analyzed in the previous section.

In order to obtain the dominant spectral components present during the last ice age, we performed a Fourier analysis of time intervals I and II of GISP2  $\delta^{18}\text{O}$  record, as it was previously done for the Holocene. The first part of the GISP2  $\delta^{18}\text{O}$  record has an average time interval of  $\sim 322$  years. After a linear interpolation the time interval has a fixed value of  $\sim 45$  years. The interpolated signal contains  $N = 1338$  data points. When performing the Fourier analysis we added 15 662 zeros at the end of the data array for increasing the frequency resolution. As a result we obtained a group of four dominant spectral components: (13421, 7886, 5238, 4026) years.

The second part of the GISP2  $\delta^{18}\text{O}$  record has an original average time interval of  $\sim 100$  years. After the interpolation the time interval is  $\sim 22$  years. The interpolated signal has  $N = 1729$  data points and we added 15 271 zeros at the end of the data array. We have used the Hanning function for both Fourier spectra. In this part we obtained a group of four dominant spectral components: (8500, 4617, 2992, 1433) years.

The analyses of these records reveal that the dynamic of temperature during the last ice age is ruled by the transitions between the cold and the warm state. In order to understand this dynamic, we calculated the distance between a vector composed by the dominant spectral components and their amplitudes (for each part of GISP2 record) and those obtained from simulations following a procedure similar to the one sketched for the Holocene.

In Fig. 4 we observe the ensemble-average ( $\langle d \rangle$  in panel a) and minimum distance ( $\langle d \rangle_{>10\text{min}}$  and  $d_{\text{min}}$  in panel b) between the simulations and the experimental spectra as a function of noise amplitude, together with experimental and simulated time series (panel c) and Fourier spectra (panel d) for the first part of ice age. The ensemble-average minimum, observed for  $D = 0.2$ , points out the region in which a vast majority of events display a Fourier spectra similar to the experimental one. The frequency spectra plotted in panel (d) corresponds to the event who minimizes this distance. We can appreciate the notorious similarities between the experimental and the simulated spectra.

In Fig. 5 we plot the same quantities for the second part of the ice age. This part of the ice age is particularly interesting because the dominant spectral component is approximately 1470 years. A minimum value in the ensemble-average distance points out a range of noise where the ensemble of the simulated spectra is close to the experimental one. It can be observed that there is a slight difference between the minimum of the ensemble-average and the minimum distance. This difference is due to the dispersion found in Fourier spectra in this dynamical regime. While the ensemble-average distance minimizes for  $D = 0.41$ , the minimum distance does for  $D = 0.385$ . The simulated Fourier spectra displayed in panel d corresponds to  $D = 0.385$

It is important to notice that even though the dominant spectral component is  $\sim 1470$  years, the dynamical regime of the model which better fits the experimental Fourier spectra

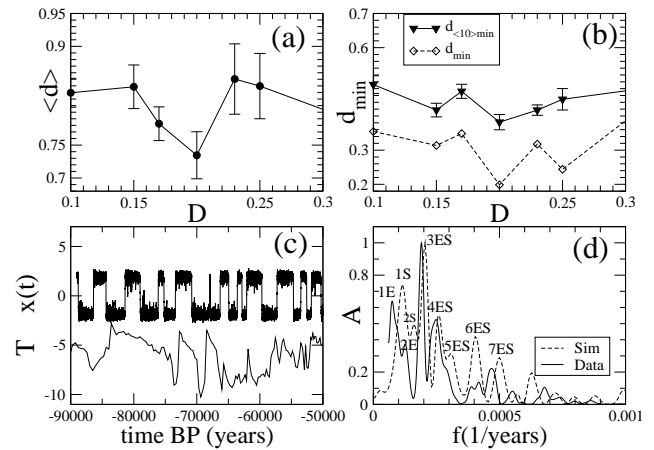


**Fig. 4.** First Part of the Ice Age: ensemble-average (panel a) minimum distance and average over the ten smallest distances (panel b) between simulations and experimental spectra as a function of noise amplitude, together with experimental and simulated time series (panel c) and Fourier spectra (panel d). The noise amplitude used in panels c and d is  $D = 0.2$ .

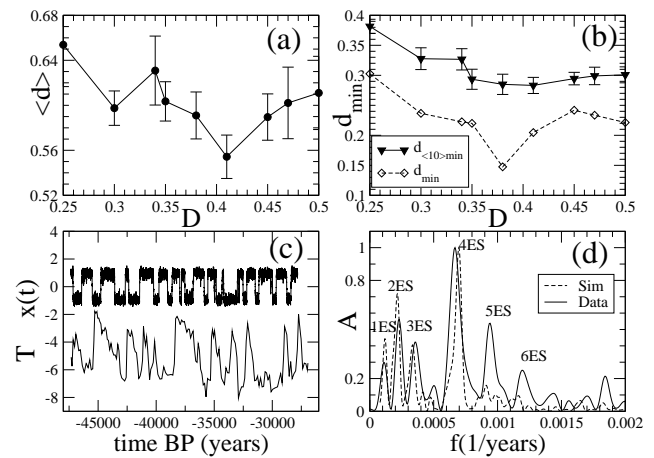


**Fig. 5.** Second Part of the Ice Age: ensemble-average (panel a) minimum distance and average over the ten smallest distances (panel b) between simulations and experimental spectra as a function of noise amplitude, together with experimental and simulated time series (panel c) and Fourier spectra (panel d). The noise amplitude used in panels c and d is  $D = 0.385$ .

does not corresponds to the ghost stochastic regime (GSR). Simulations not shown in this manuscript reveal that in the GSR, the peak of 1470 years in the frequency spectra is absolute dominant (low frequency spectral components are not present in the spectrum) and the dispersion among events is minimum.

In Table 2 we can observe a full comparison between the experimental data and the simulations for the whole ice age, as well as an interpretation in terms of the forcing auto-correlation function. The notorious agreement between the

**Table 2.** Labels (first column), main periods obtained from the GISP2  $\delta^{18}\text{O}$  record (second column), autocorrelation maxima for the solar forcing (F.A.M, third column) and main periods obtained from the simulations, for time interval I (early ice age) (top) and time interval II (late ice age) (bottom). Simulations noise amplitudes are  $D = 0.1125$  (time interval I) and  $D = 0.385$  (time interval II). The highlighted periods correspond to the dominant spectral component in each time interval.

| Time interval I (early ice age) |              |                    |             |
|---------------------------------|--------------|--------------------|-------------|
| Label                           | Experimental | F.A.M.             | Simulations |
| 1E                              | 13 421       | $\sim 13\,415$     | –           |
| 1S                              | –            | $\sim 8775$        | 8665        |
| 2E                              | 7886         | $\sim 7900$        | –           |
| 2S                              | –            | $\sim 6050$        | 6239        |
| 3ES                             | <b>5238</b>  | $\sim$ <b>5260</b> | <b>4875</b> |
| 4ES                             | 4026         | $\sim 4030$        | 3900        |
| 5ES                             | 3484         | $\sim 3335$        | 3249        |
| 6ES                             | 2391         | $\sim 2285$        | 2475        |
| 7ES                             | 2137         | $\sim 2105$        | 2000        |
| Time interval II (late ice age) |              |                    |             |
| Label                           | Experimental | F.A.M.             | Simulations |
| 1ES                             | 8500         | $\sim 8510$        | 9175        |
| 2ES                             | 4617         | $\sim 4645$        | 4332        |
| 3ES                             | 2992         | $\sim 2900$        | 2785        |
| 4ES                             | <b>1433</b>  | $\sim$ <b>1486</b> | <b>1499</b> |
| 5ES                             | 1097         | $\sim 1050$        | 1061        |
| 6ES                             | 860          | $\sim 875$         | 839         |

experimental data and the simulations can be understood under the hypothesis that the temperature dynamic during this age is completely determined by transitions between the cold and the warm states driven by the periodic function composed by the De Vries/Suess and Gleissberg tones. The resident times coincide with the autocorrelation function maxima, according to what is expected in a threshold dynamical system when stimulated with sub-threshold complex functions plus noise (Chialvo, 2003; Balenzuela and García-Ojalvo, 2005). This fact stresses the importance of this mechanism as responsible for the system's dynamic during this age.

These results let us think about the possibility to relate the first part of the GISP2  $\delta^{18}\text{O}$  record as a regime characterized by a low noise amplitude and consequently to a low probability of transition between states. Moreover, we may think that the second part of the GISP2  $\delta^{18}\text{O}$  record is characterized by a better fit between the forcing, the threshold and the noise amplitude. This means that the system is closer to (but not into) a near 1470 years resonance (Chialvo, 2003; Balenzuela and García-Ojalvo, 2005).

A natural question that arises from these results is how do they depend on the choice of the parameters. In this simple model, the whole dynamics is ruled by the interplay between

forcing, threshold and noise. For this threshold behavior, which is one of the hypothesis of the model as we explained above, the election of the amplitude forcing value in the onset of transition ( $F = 0.2265$ ) is the one that allows the model to reproduce the largest scenario of recorded data (the whole ice age and the Holocene) changing the minimum amount of parameters: just the noise amplitude. Moreover, this parameter election produces a robust matching between data and simulations in the sense that most of the events of a given ensemble show Fourier spectra similar to the corresponding to paleo-temperature data in each analyzed stage, as can be deduced from the minimum of the ensemble-averaged distance. If we change the value of the forcing amplitude  $F$ , the model will not be able to reproduce the results corresponding to the Holocene age, in which the different frequency components arise from the interplay between the forcing and the nonlinearities of the potential. If the amplitude  $F$  is considerably lower than  $F = 0.2265$ , lets say  $F = 0.1$ , the system will be placed in the low oscillation regime and it will be necessary a larger noise amplitude in order to produce transitions between both stable states. Results not shown in this paper indicate that the matching with recorded data is much worse if  $F = 0.1$  as the one shown in Figs. 4 and 5. The larger noise levels that are necessary in this regime, in order to trigger transitions between both states, produce more dispersion in the Fourier spectra of the member of a given ensemble, making the model's behavior less robust. On the other hand, if we take a value of  $F$  considerably greater than  $F = 0.2265$ , lets say  $F = 0.3$ , the system switches between the stable states in absence of noise and therefore it is unable to reproduce the behavior of the early ice age dominated by a  $\sim 5000$  years spectral component. However, with this forcing amplitude and an appropriate value of the noise amplitude, the model could be able to reproduce a similar matching for the late ice age than those obtained in Fig. 5 for  $F = 0.2265$ .

A final discussion concerning the role of the noise should be addressed before reaching the conclusions. D-O events are very often regarded as being forced by anomalies in the freshwater flux of the North-Atlantic ocean (Ganopolski and Rahmstorf, 2001). A very plausible source of noise-like freshwater anomalies in the North-Atlantic area which are the adjacent ice sheet. Since the volume of these ice sheets was considerably larger during glacial times that during the present Holocene, it appears to be quite plausible to assume that noise level was much larger during the last ice age than during the Holocene, as we observe in the simulations.

## 5 Conclusions

In this work, we have developed a conceptual model based on the key assumptions of a more complex model, the CLIMBER-2 and inspired by the conceptual model analyzed in (Braun et al., 2007). We have found that the interplay between the forcing function (a complex periodic signal composed with frequencies of the De Vries/Suess and Gleissberg

cycles) and the nonlinearities of the potential give rise to a complex dynamical behavior in the onset of transitions whose spectral components has been reported in the analysis of  $\delta^{18}\text{O}$  and  $^{14}\text{C}$  during the Holocene. This analysis gives a plausible explanation for the spectral components observed in Holocene's records which can not be associated to known solar cycles. The simplicity of the model, however, avoids an exact coincidence between Fourier spectra of simulations and experimental data during the Holocene.

We have also shown that simply by varying the noise amplitude in order to allow transitions from one stable state to the other, the model is able to reproduce the main features of Fourier spectra of temperature records during the last ice age. We have seen that, according to the performed simulations, the main spectral features of this stage corresponds to two different dynamical regimes and can be understood in terms of transitions between cold and warm states. When transitions take place, the dominant spectral components in the dynamics of the system could be understood in terms of forcing's autocorrelation function, as we have seen in Table II. The specific nonlinearities of the model are not relevant in this dynamical regime. This is the reason behind the best agreement between the simulations and experimental data during the last ice age compare to the Holocene.

This framework supports the idea of the main role that the solar forcing plays in relation to the behavior of global climate and establish a plausible scenario to understand temperature variations in Greenland paleo-climate records as an interplay between the De Vries/Suess and Gleissberg cycles and the nonlinearities of the climate system.

Finally, it is important to notice that, despite the GISP2 data shows an apparently significant spectral component of 1470 years (Schulz, 2002) during the interval 12–50 kyr BP, the best fitted simulations for this stage does not correspond to a Ghost Stochastic Resonance regime, although they are close to it.

*Acknowledgements.* This work was partially supported by Grant X-404 from University of Buenos Aires.

Edited by: V. Perez-Munuzuri

Reviewed by: N. Lorenzo and M. D. Dima

## References

- Balenzuela, P. and García-Ojalvo, J.: Neural mechanism for binaural pitch perception via ghost stochastic resonance, *Chaos*, 15, 023903–023910, 2005.
- Bond, G. C., Showers, W., Elliot, M., Evans, M., Lotti, R., Hajdas, I., Bonani, G., and Johnson, S.: Mechanisms of Global Climate Change at Millennial Time Scales, AGU, Washington, DC, *Geophys. Monogr.*, 112, 35–58, 1999.
- Braun, H., Christl, M., Rahmstorf, S., Ganopolski, A., Mangini, A., Kubatzki, C., Roth, K., and Kromer, B.: Possible solar origin of the 1470-year glacial climate cycle demonstrated in a coupled model, *Nature*, 438, 208–211, 2005.
- Braun, H., Ganopolski, A., Christl, M., and Chialvo, D. R.: A simple conceptual model of abrupt glacial climate events, *Nonlin. Processes Geophys.*, 14, 709–721, doi:10.5194/npg-14-709-2007, 2007.
- Braun, H., Ditlevsen, P., and Chialvo, D. R.: Solar forced Dansgaard-Oeschger events and their phase relation with solar proxies, *Geophys. Res. Lett.*, 35, L06703–L06707, doi:10.1029/2008GL033414, 2008.
- Chialvo, D. R.: How we hear what is not there: A neural mechanism for the missing fundamental illusion, *Chaos*, 13, 1226–1230, 2003.
- Crowley, T. J. and Kwang-Yul, K.: Towards development of strategy for determining the origin of decadal-centennial scale climate variability, *Quaternary Sci. Rev.*, 12, 375–385, 1993.
- Dima, M. and Lohmann, G.: Conceptual model for millennial climate variability: a possible combined solar-thermohaline circulation origin for the  $\sim 1500$ -year cycle, *Clim. Dynam.*, 32(2–3), 301–211, 2009.
- Ganopolski, A. and Rahmstorf, S.: Simulation of rapid glacial climate changes in a coupled climate model, *Nature*, 409, 53–158, 2001.
- Gammaitoni, L., Hanggi, P., Jung, P., and Marchesoni, F.: Stochastic resonance, *Rev. Mod. Phys.*, 70, 223–288, 1998.
- García-Ojalvo, J. and Sancho, J. M.: *Noise in Spatially Extended Systems*, Springer, New York, 1999.
- Karlen, W. and Kuylenstierna, J.: On solar forcing of Holocene climate: evidence from Scandinavia, *The Holocene*, 6(3), 359–365, 1996.
- O'Brien, S. R., Mayewski, P. A., Meeker, L. D., Meese, D. A., Twickler, M. S., and Whitlow, S. I.: Complexity of Holocene climate as reconstructed from a Greenland ice core, *Science*, 270, 1962–1964, 1995.
- Peristykh, A. N. and Damon, P. E.: Persistence of the Gleissberg 88-year solar cycle over the last  $\sim 12\,000$  years: Evidence from cosmogenic isotopes, *J. Geophys. Res.*, 108, 1003–1017, doi:10.1029/2002JA009390, 2003.
- Schulz, M.: On the 1470-year pacing of Dansgaard-Oeschger warm events, *Paleocoenography*, 17(2), 1014–1022, doi:10.1029/2000PA000571, 2002.
- Sonett, C. P., Finney S. A. and Berger A.: The Spectrum of Radiocarbon [and Discussion], *Philos. T. R. Soc. Lon. A*, 330, 413–426, 1990.
- Stuiver, M. and Braziunas, T. F.: Sun, Ocean, Climate and Atmospheric  $^{14}\text{C}$ , an evaluation of causal and spectral relationships, *The Holocene*, 3, 289–305, 1993.
- Stuiver, M., Braziunas, T. F., and Grootes, P. M.: Is There Evidence for Solar Forcing of Climate in the GISP2 Oxygen Isotope Record?, *Quaternary Res.*, 48, 259–266, 1997.
- Wagner, G., Beer, J., Masarik, J., and Muscheler, R.: Presence of the solar De Vries cycle ( $\sim 205$  years) during the last ice age, *Geophys. Res. Lett.*, 28, 303–306, 2001.
- ZhiQiang, Yin, LiHua, Ma, YanBen, Han, and YongGang, Han: Long-term variations of solar activity, *Science China Press*, 52, 2737–2741, 2007.